

Swelling of couscous grains under saturated conditions^{★,★★}

Sébastien KIESGEN DE RICHTER^{a,*2}, Naïma GAUDEL^{b,1}, Claire GAIANI^{b,2},
Arthur PASCOT^a, Maude FERRARI^a and Mathieu JENNY^a

^aUniversité de Lorraine, LEMTA, CNRS UMR 7563, F-54000 Nancy, France

^bUniversité de Lorraine, LIBio, F-54000 Nancy, France

ARTICLE INFO

Keywords:

Couscous grains
Swelling
MRI measurements

Abstract

The article presents a grain-scale experimental approach for the study of a model that swells granular food material. During the swelling phase, both the evolution of particle size using image analysis and the spatially resolved field of diffusion coefficient of water inside the grains were studied using MRI measurements. A concentrically penetration of water in the cross section of the grains was shown on images. The experimental results were compared to classical models from the literature used to predict the swelling of polymeric materials. A simple first-order kinetic equation was shown to be adequate to describe the size evolution during swelling. Thus, the results suggested that the swelling dynamics was a water uptake-limiting mechanism because of the existence of a gelatinous layer at the grain surface formed during the manufacturing process, as previously reported in the literature.

1. Introduction

The swelling of a granular particle is a spontaneous increase in its volume to restore the equilibrium between the solid phase and the surrounding fluid[1, 8, 12]. The initial out-of-equilibrium condition originates from a change in the particle environment or a change in the chemical conditions of the interstitial fluid (composition, salinity, etc.). This phenomenon is associated with a complex hydro-mechanical coupling where the evolution of the solid matrix modifies the distribution of the liquid in the pores, which in turn modifies the swelling rate[10, 30, 39]. Therefore, the absorption of a single particle depends on a number of parameters such as molecular structure, inner surface, porosity, hydrophobicity or crosslinking of the solid matrix.

Swelling in saturated conditions occurs in many industrial processes and environmental phenomena. For example, the swelling of clays that modifies the stability of soils[4, 27, 32], or the swelling of hydrogel in hygienic products[9]. In addition, this phenomenon is a key step in food engineering[41, 43, 44] because it influences many mechanisms, such as powder reconstitution, agglomeration or frying[41]. In practical conditions, the reconstitution of food powders involves a number of steps that often overlap: wetting, sinking, swelling, dispersion, and solubilization[13, 15, 26, 34], making it difficult to characterize each step individually. It is then impossible to give a general rule for the influence of both the hydro-mechanical coupling and physicochemical properties of powders on the reconstitution process. A

* This study was conducted in the framework of the "PowderReg" project, funded by the European programme Interreg VA GR within the priority axis 4 "Strengthen the competitiveness and the attractiveness of the Grande Région / Großregion".

** This research was also supported by a grant from the International Fine Particle Research Institute (IFPRI).

*Corresponding author: [sebastien.kiesgen@univ-lorraine.fr](mailto:sbastien.kiesgen@univ-lorraine.fr)

ORCID(s): 0000-0002-7513-6709 (S.K.D. RICHTER); 0000-0002-3961-4312 (N. GAUDEL); 0000-0003-0434-8453 (C. GAIANI)

¹Present address: National Institute of Research and Safety (INRS, Nancy, France)

²Institut Universitaire de France

16 better understanding of the basic physical mechanisms involved in the swelling of food granular media is therefore
17 necessary.

18 Among granular media in food, couscous grains have the advantage of being well controlled in size, shape and
19 composition[2]. In particular, this grain allows the study of swelling as it limits the dispersion of its solid matrix dur-
20 ing its reconstitution. This makes it a model system for studying the swelling of granular food materials. Moreover,
21 couscous powders are of major industrial interest since they are one of the most common food products made from
22 durum wheat[17]. Couscous grains are obtained after wet agglomeration, rolling-sieving, steam cooking, and drying
23 [3]. The wet agglomerates are formed by mixing durum wheat semolina and water together to induce the wet agglom-
24 eration of the native semolina particles. These wet agglomerates are rolled in a rotating screen drum to homogenize
25 the structure and size of the grains (between 1 and 2 mm). To strengthen the structure, the rolled agglomerates are
26 then cooked. Finally, they are dried to reduce their water content and to maintain their stability during storage.

27 Couscous particles are thus mainly composed of starch granules bound by a gluten matrix[16], sometimes includ-
28 ing aleurone cells with an alveolar structure[18]. These particles are millimetric in size, are almost spherical and
29 begin to absorb water by capillary diffusion when poured into a liquid. Water diffusion into particles induces particle
30 swelling due to the relaxation of polymer chains[31, 36], which softens the particle, increases its size and decreases its
31 mechanical resistance to shear stresses[14, 28, 35]. Wetting is generally improved for large particles and agglomerates,
32 as well as for more spherical particles[19, 24], as they offer lower particle-solvent contact angles than small particles.
33 Highly porous particles are also known to display a better wetting behavior, as water mass transfer into the particle is
34 enhanced by water uptake in the pores[16, 22].

35 A range of studies have been performed to model the swelling of granular particles[8, 33, 45]. Most of them are
36 semi-empirical[11, 29] and show evidence that swelling properties depend on particle size and composition. Recently,
37 Sweijden et al.[39] proposed a physical model to predict the swelling of Super Absorbent Polymer (SAP) particles.
38 This model is based on a free diffusion of water in particles and has been generalized to take into account irregular
39 particle shape and water uptake on the surface[25]. This model successfully predicts the swelling of pharmaceutical
40 particles[37] or SPA particles[39] under saturated conditions, but has never been applied to food powders. Particle
41 swelling mainly depends on the water diffusion coefficient D and the maximum absorption ratio Q_{max} , defined as the
42 ratio between the mass of the hydrated and the dry particles. An open question is how these two parameters depend
43 on the size, morphology and chemical composition of the particles. Although Q_{max} can be measured experimentally
44 using simple weighing methods, in many situations the direct determination of the value of D is much more difficult;
45 nonetheless, it is crucial since it is considered as constant in many models.

46 To summarize, there is currently no physical model to predict the swelling of granular food materials from the
47 mechanical and physicochemical properties of the grains and their environment. The swelling mechanism is complex

Table 1

Chemical composition of couscous grains used in this study.

Ingredient	Composition (% of dry matter)
Carbohydrates	72 %
Proteins	12 %
Fat	1.8 %
Fibers	2.4 %
Minerals	0.04 %

48 because of the coupling between the evolution of the liquid flow properties on the one hand and the evolution of the
 49 chemical nature and mechanical properties of the solid matrix on the other. Yet, predicting the swelling of couscous
 50 grain and of any granular grain for food processing is important, for at least two reasons. First, to **achieve** the precise
 51 nutritional, physical, chemical and sensorial properties of couscous products, it is particularly important to deepen
 52 knowledge of the structure-function relationship between the grains and water. Secondly, via the swelling process,
 53 these particles can take up water and thus open up a variety of new formulation applications for valuable products.

54 In this article, time-resolved optical measurements of the swelling dynamics of couscous particles under saturated
 55 conditions **were combined** with spatially resolved Magnetic Resonance Imaging (MRI) measurements at the grain scale
 56 to evaluate the diffusing properties of water. To the best of the authors' knowledge, little use has been made of MRI
 57 in food products to date, and even less on food powders such as couscous grains[23]. However, MRI offers numerous
 58 opportunities for monitoring water uptake and water distribution in these products. **The results were** then directly
 59 compared with the theoretical predictions from the literature related to the swelling of SAP particles. The relevance
 60 of such an approach to predict the swelling of granular media in food **was then discussed**.

61 2. Materials and methods

62 2.1. Materials

63 In this study, couscous powder made of industrial durum wheat semolina (Comptoir du Grain, Arles, France) **was**
 64 **used** (see Tab. 1). The bulk density value, measured in triplicate with a pycnometer, was $\rho_s = 1380 \pm 5 \text{ kg.m}^{-3}$ at 20 °C.
 65 The surface structure of the grains was obtained using Scanning Electron Microscopy, SEM type JEOL JSM-7100F133
 66 supplied with a hot (Schottky) electrongun (JEOL Ltd., Tokyo, Japan) from $\times 600$ to $\times 9000$ magnification in a partial
 67 vacuum using 3 kV accelerating voltage. Prior to analysis, the samples were coated with carbon in a sputter coater
 68 (Polaron SC7640, Thermo VG Scientific, East Grinstead, United Kingdom). Particle size distribution was determined¹
 69 using a laser diffraction granulometer (Mastersizer 3000, Malvern Instruments, UK) in the range 0.1 – 3500 μm .

70 Fig. 1 shows the SEM images and the particle size distribution. The median size of the couscous particle was

¹Classical granulometric parameters were determined: d_{10} , d_{50} , and d_{90} , corresponding to the diameters for which 10 %, 50 %, and 90 % of the particle population have smaller sizes, and the span, a polydispersity indicator defined as the width of the distribution normalized by its median: $span = \frac{d_{90}-d_{10}}{d_{50}}$

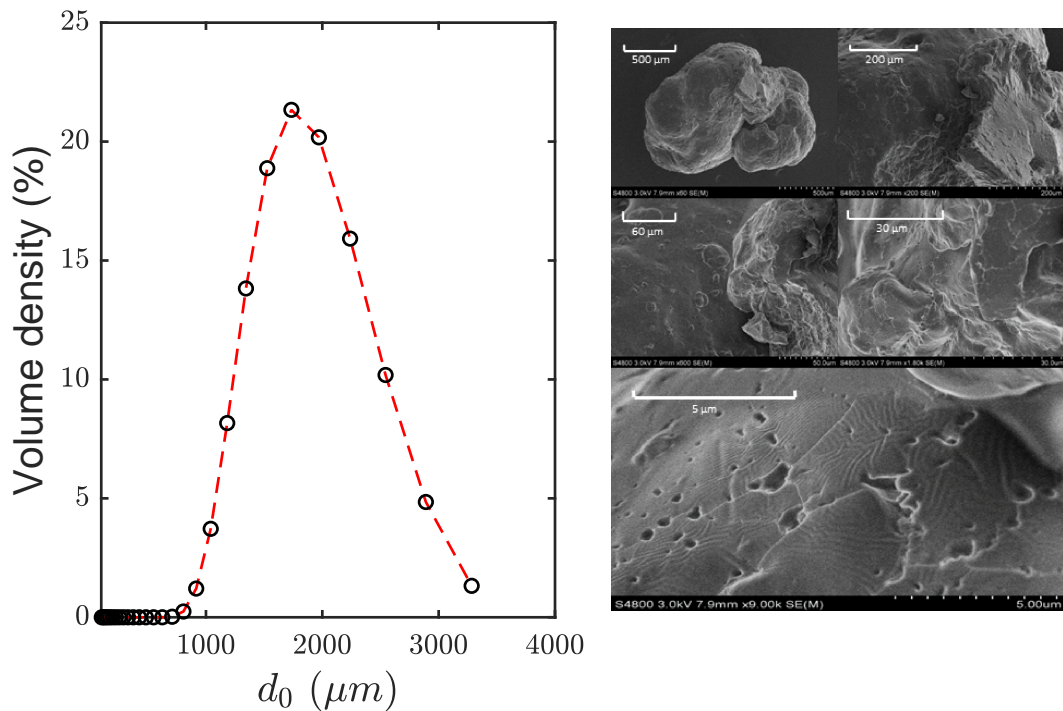


Figure 1: Left: Particle size distribution of couscous grains. The volume density defined in terms of equivalent sphere diameter (%) is shown as a function of particle diameter d_0 . Right: SEM images from $\times 600$ to $\times 9000$ magnification in a partial vacuum using 3 kV accelerating voltage.

⁷¹ $d_{50} = 1700 \mu\text{m}$, and the size distribution was slightly polydisperse (*span* = 0.7). The maximum absorption ratio
⁷² of single particles (Q_{max}), defined as the ratio between the mass of the swollen particle and the mass of the dry
⁷³ particle, was estimated after two hours by vacuum filtration. In deionized water at 20 °C ($\rho_w = 10^3 \text{ kg.m}^{-3}$), the
⁷⁴ value of Q_{max} was found to be equal to $Q_{max} = 3.54 \pm 0.41$. The sphericity and aspect ratio results suggested that the
⁷⁵ particles of couscous powders had quasi spherical shapes. Since the grains only differ by their median size, as shape
⁷⁶ parameters, chemical compositions, water activities, maximum absorption ratio, densities, and surface appearance
⁷⁷ (porosity, roughness), all the grains were used in the distribution, with no preliminary sieving, in the subsequent
⁷⁸ phases.

⁷⁹ 2.2. Methods

⁸⁰ 2.2.1. Optical measurements and image analysis

⁸¹ A CCD camera (Lumenera Lw235M 2.0 Megapixel, $1616 \times 1216 \text{ pix}^2$), placed at the bottom of a transparent
⁸² PMMA vessel, recorded the swelling dynamics of single particles through a 45° tilted mirror. The acquisition frequency

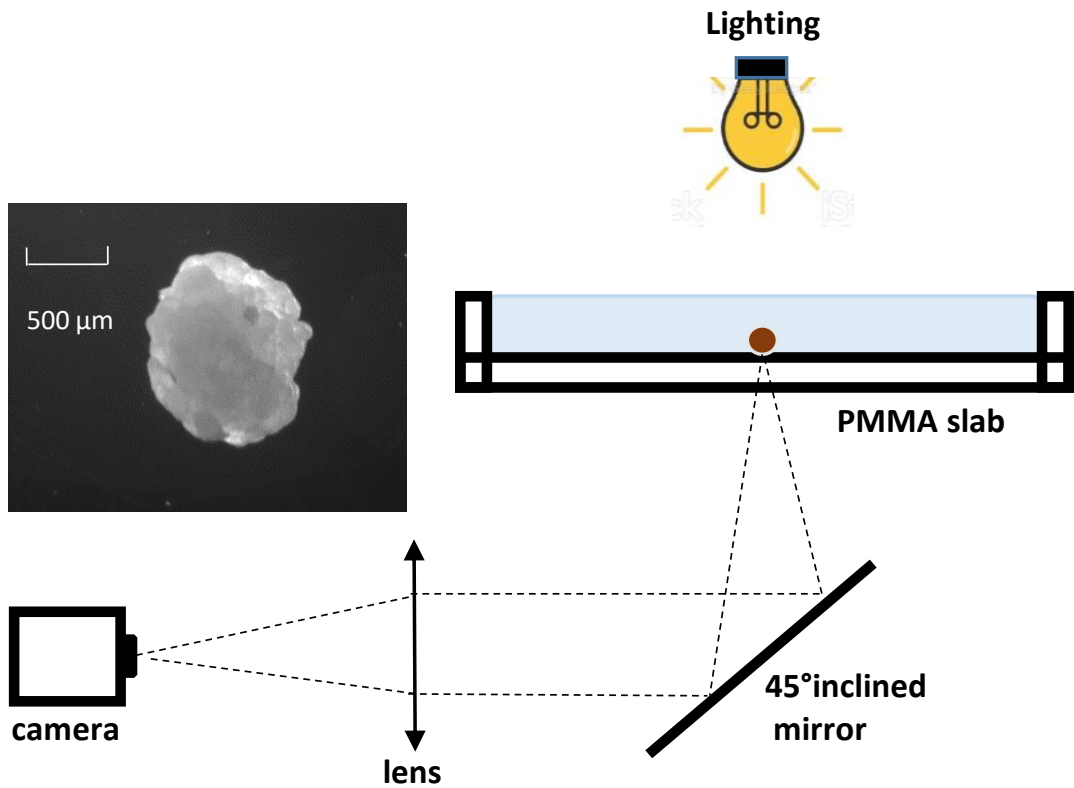


Figure 2: Sketch of the experimental setup used to follow the swelling of a single couscous grain.

of the camera was 30 Hz and the grain was illuminated from above with a LED projector. A sketch of the experimental setup and a typical image are given in Fig. 2. From the recorded images, data processing using the ImageJ software [20] was applied to analyze and quantify the swelling of single particles. The images were first binarized by thresholding to obtain grains that appeared as white spots on a dark background. The edge and centroid of the particles were then detected. A calculation of the distance between the centroid and the edge of the particles returned object properties (area, perimeter, minor axis, major axis of fitted ellipsoid). In the following, particle diameter $d(t)$ denotes twice the mean distance between the centroid and the edge of the particle at time t during swelling.

2.2.2. Magnetic Resonance Imaging measurements

To map the diffusion coefficient D of water molecules in the grains during swelling, a magnetic resonance imaging (MRI) technique was used [38, 42]. This spectroscopy technique is non-intrusive, and is used to see through opaque materials and monitor dynamic phenomena by direct marking (no tracer injection). The swelling was tracked by direct detection of the water protons at the grain scale. The MRI experiments were carried out with a Bruker Avance III 600 wide bore spectrometer (14.1 T, 600 MHz proton resonance frequency, Bruker, Germany). The sample temperature

96 was regulated to 20 ± 0.1 °C. The micro-imaging probe (MicWB40) was a 25 mm quadrature resonator manufactured
 97 by Bruker, with a 150 G.cm^{-1} gradient system. Although MRI is a unique technique in providing information on the
 98 changes in distribution of water within and outside the couscous grains, assigning the relaxation times remains a major
 99 difficulty regarding the signal to noise ratio if [the swelling dynamics at short time scales has to be captured](#). In fact,
 100 the measured single relaxation time, $T1$, in couscous grains after swelling was of the order of 2 s. This value makes
 101 it very difficult to obtain proton weighted images at short times during swelling. Thus, in this study, proton density
 102 images were only used to qualitatively illustrate the evolution of the particle size over time as well as the position of
 103 the liquid interface during water penetration at the beginning of the swelling. To extract quantitative data, [a diffusion-](#)
 104 [weighted sequence based on a signal difference was used](#), which allowed [the extraction of the diffusion coefficient value](#)
 105 minimizing the relaxation effects. The acquisition of proton density images was performed using a standard spin-echo
 106 sequence with an echo time of 14 ms and a repetition time² of 500 ms. The geometric parameters were as follows:
 107 the field of view (FOV) was $2.5 \text{ cm} \times 2.5 \text{ cm}$, the thickness slide was $500 \mu\text{m}$, and the image size was $256 \times 256 \text{ pix}^2$.
 108 The acquisition of each point lasted about 2 min and the images obtained had a spatial resolution of about $98 \mu\text{m}$.
 109 The apparent diffusion coefficient (mean of D at the voxel scale) can be measured by MRI using a diffusion-weighted
 110 sequence (PFGSE for pulsed field gradient spin echo). The PFGSE sequence consisted of the application of two
 111 gradients of short and intense magnetic fields. The first one gave the proton precession a phase advance according to
 112 their position, and the second compensated for this advance. Thus, only immobile protons underwent a zero phase
 113 shift. With this sequence, the spin-echo attenuation S was related to the intensity of the magnetic field gradient G , via
 114 Eq.1:

$$S = A \exp \left[-\gamma^2 \delta^2 \left(\Delta - \frac{\delta}{3} \right) D G^2 \right] \quad (1)$$

115 where γ is the nuclear gyro-magnetic ratio, $\delta = 6 \text{ ms}$ is the duration of the diffusion gradient, A the amplitude of the
 116 signal and $\Delta = 11 \text{ ms}$ is the evolution time (delay between the two gradients). S was fitted to Eq.1 for each swelling
 117 time point to extract a mapping of the self-diffusion coefficient D for ten gradient values (see fig.6 (b)). The geometric
 118 parameters were then as follows: the field of view (FOV) was $2.5 \text{ cm} \times 2.5 \text{ cm}$, the thickness slide was $500 \mu\text{m}$, and
 119 the image size was $128 \times 128 \text{ pix}^2$. The acquisition of each point lasted about 2 min and the images obtained had a
 120 spatial resolution of about $200 \mu\text{m}$. To validate our protocol, [it has been checked for each experiment that the diffusion](#)
 121 [coefficient of pure water was found](#) outside the grains showing that [the \$T1\$ and \$T2\$ relaxation times were not limiting](#).

²The value of the repetition time [was](#) a compromise between the duration of the experiments and the signal to noise ratio to ensure both good image quality and good [time](#) resolution.

122 **3. Results and discussions**

123 **3.1. Evolution of particle diameter**

124 In the following, all swelling experiments were performed in deionized water at 20 °C. Working at room temperature
 125 allowed swelling to take place over long periods of time and was particularly well suited to the low time resolution of
 126 the MRI methods.

127 The swelling typically lasts 3 hours in the experimental conditions presented in this study (Fig. 3), and the ratio
 128 between the final and the initial diameters is constant ($d_{max}/d_0 = 1.6 \pm 0.1$), as shown in Fig. 4, left. It can be seen
 129 in the inset of Fig. 3 that the shape remains globally identical, as confirmed by the measurements of the sphericity
 130 coefficient e , defined as $e = 4\pi S_g/p^2$ where S_g and p are the area of the grain and its perimeter at time t , respectively
 131 (see Fig. 4, right). A value of e close to 1 confirms the hypothesis of the grains being almost spherical in the rest of
 132 the analysis.

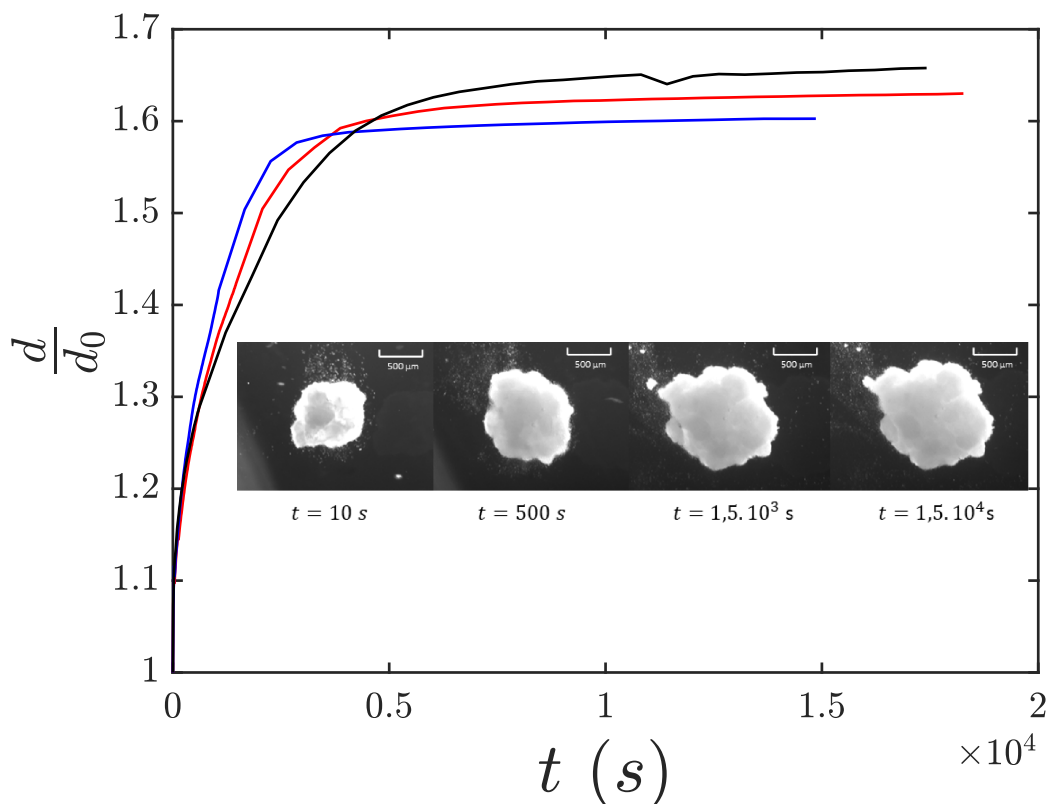


Figure 3: Typical time evolution of the normalized diameter d/d_0 . The curves correspond to different initial diameter d_0 . $d_0 = 1.37$ mm, 1.63 mm and 1.90 mm for the blue, red and black curves, respectively. Inset: typical images of a couscous particle at different times during swelling, recorded with a CCD camera.

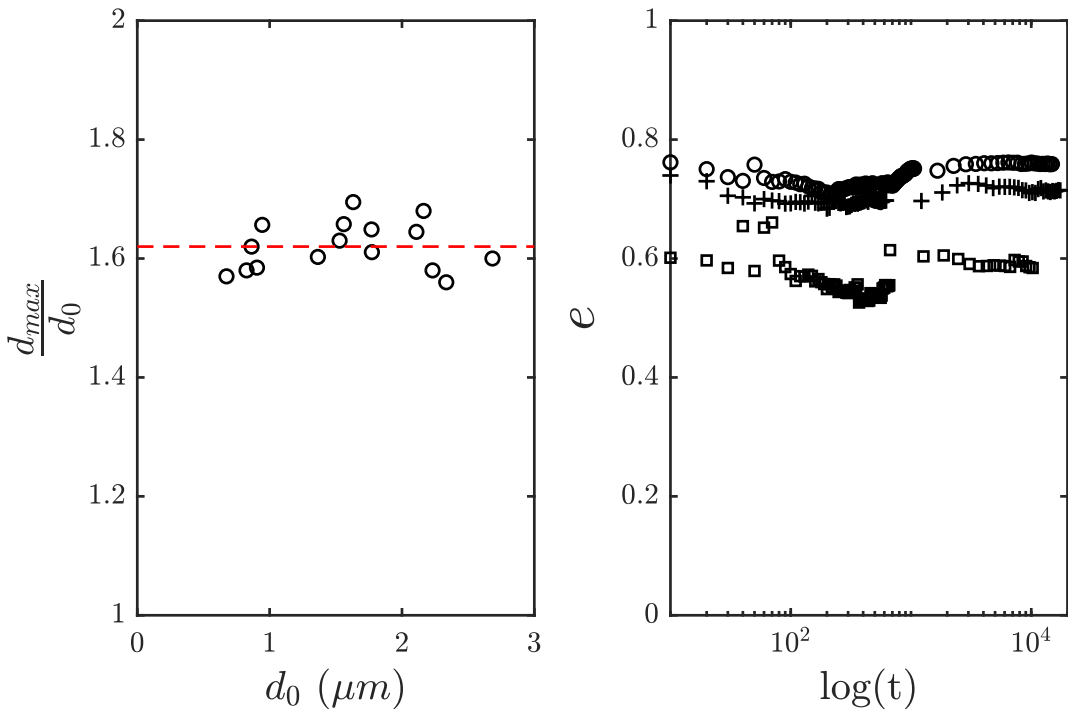


Figure 4: Left: Evolution of the normalized maximal diameter d_{max}/d_0 as a function of the initial diameter d_0 . Right: Typical time evolution of the circularity parameter e during swelling for four independent experiments.

3.2. Water diffusion in grains

The distribution of water inside the grains was followed using Magnetic Resonance Imaging (MRI) of proton density and linked to the evolution of their diameter. Fig. 5 shows the long-time swelling dynamics of five couscous grains over a total period of 30 hours. As expected, the water diffuses from the edges towards the center of the grains during the swelling period, which is about 3 hours. Swelling occurs when water is not able to penetrate to the center of the aggregates and disrupts the structure by hydration of the sub-particles. After this time, the grain size no longer changes but the amount of water continues to slowly increase inside the grains until, after 30 hours, the signal is almost identical to the pure water signal.

This behavior over a long time is due to the presence of air pockets trapped in the porous matrix of the grain, which slowly dissolves in the surrounding water. As estimated by image analysis, the characteristic size of these air bubbles is $\sim 100 \mu m$, and the volume fraction is $\sim 6\%$ of the total volume of the grain once it has reached its maximum radius. The typical dissolution time of all these bubbles is of the order of ~ 15 hours, which is much greater than the time calculated from the Epstein Plessset equations (of the order of 100 s). One explanation is the fact that the trapped air

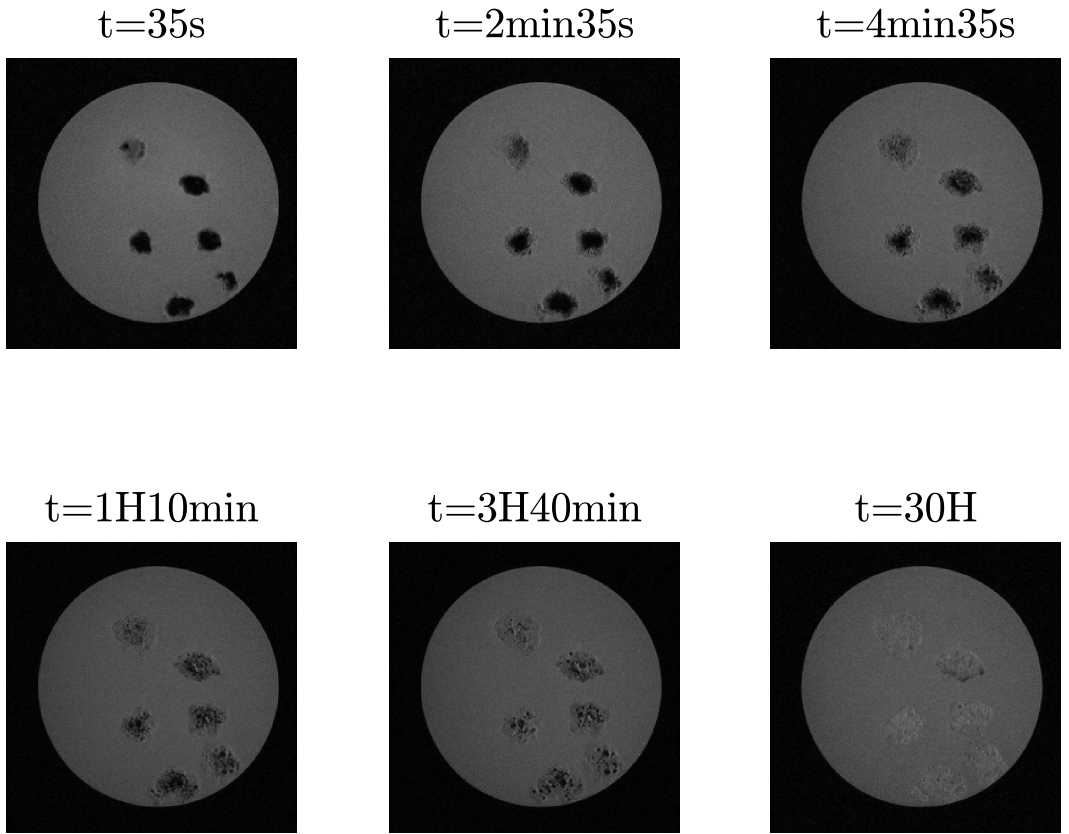


Figure 5: MRI intensity images showing the long-time swelling dynamics of six couscous grains. The image resolution is $98 \mu\text{m} \cdot \text{pix}^{-1}$.

146 has to diffuse through the gel matrix of the swollen grain, which changes the spatial scale of diffusion and increases
 147 the final dissolution time. This phenomenon of air dissolution does not influence the dynamics of swelling as such and
 148 will not be analyzed here in detail, but deserves to be mentioned.

149 From the MRI spin-echo procedure, the evolution of the attenuation signal S with the magnetic field gradient G
 150 was obtained and fitted to Eq. 1 for each pixel (see Fig. 6(a) and (b)). In Fig. 6(c), as the solid or partially wet parts of
 151 the sample returned weak signals, [those pixels for which the fit model was poor \(\$R^2 < 0.9\$ \) were eliminated](#). Then, the
 152 signal background coming from the surrounding water was [also eliminated](#) (Fig. 6(d)) making crowns appear at each
 153 time inside the particles. The mean diffusion coefficient \bar{D} was obtained by averaging the local diffusion coefficient D
 154 in the crown over all the pixels.

155 \bar{D} decreases over time during the swelling process and stabilizes when the diameter reaches its final value ($\bar{D} =$

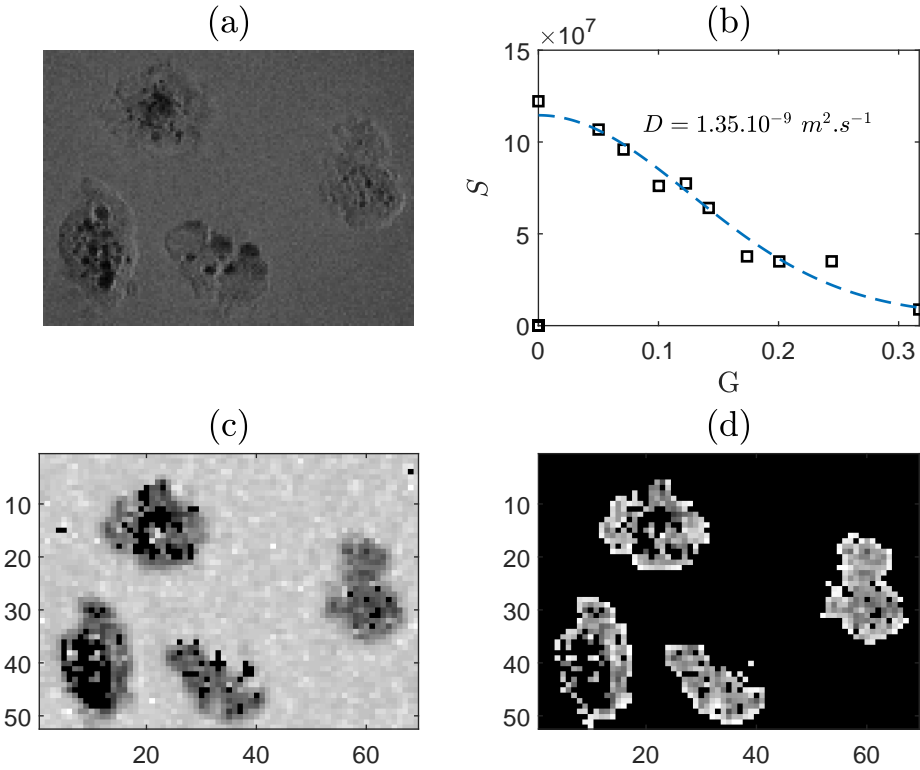


Figure 6: (a) MRI intensity image of four swollen particles at time $t = 10^3$ s. (b) Example of spin-echo attenuation at a given pixel. Data are adjusted to Eq. 1. (c) Diffusion map extracted from spin-echo attenuation of all pixels in the image. Black points correspond to pixels for which the fit model is $R^2 < 0.9$. (d) Final diffusion map by suppressing the background signal coming from the surrounding water.

156 $1.4 \cdot 10^{-9} \text{ m}^2 \cdot \text{s}^{-1}$), as shown in Fig. 7. The mapping of the diffusion fields shows that this time evolution is due to the
 157 existence of a diffusion coefficient gradient near the surface of the particles over a thickness of the order of $200 \mu\text{m}$.
 158 At any given time, the diffusion coefficient is higher in the outer ring near the surface than in the bulk of the particle.

159 3.3. Swelling models

160 In this part, the swelling dynamics extracted from experimental measurements is compared to models extracted
 161 from the literature. The swelling of individual particles is driven by the difference in chemical potential between
 162 the core of the particle and the liquid medium (deionized water in this study) [21]. It is assumed that two processes
 163 can occur during the swelling [39]: water uptake at the surface and diffusion of the liquid in the particle. These
 164 two processes may take place at the same time, or one of the two may be dominant depending on the associated
 165 characteristic times. Several works in the literature propose empirical or semi-empirical models to account for these
 166 phenomena and predict the evolution of particle diameter with time. In the following, to compare our experimental
 167 data with results from the literature, a re-scaled time is introduced (see Sweijen et al.[39]): $t^* = 4\alpha\bar{D}t/d_0^2$, where

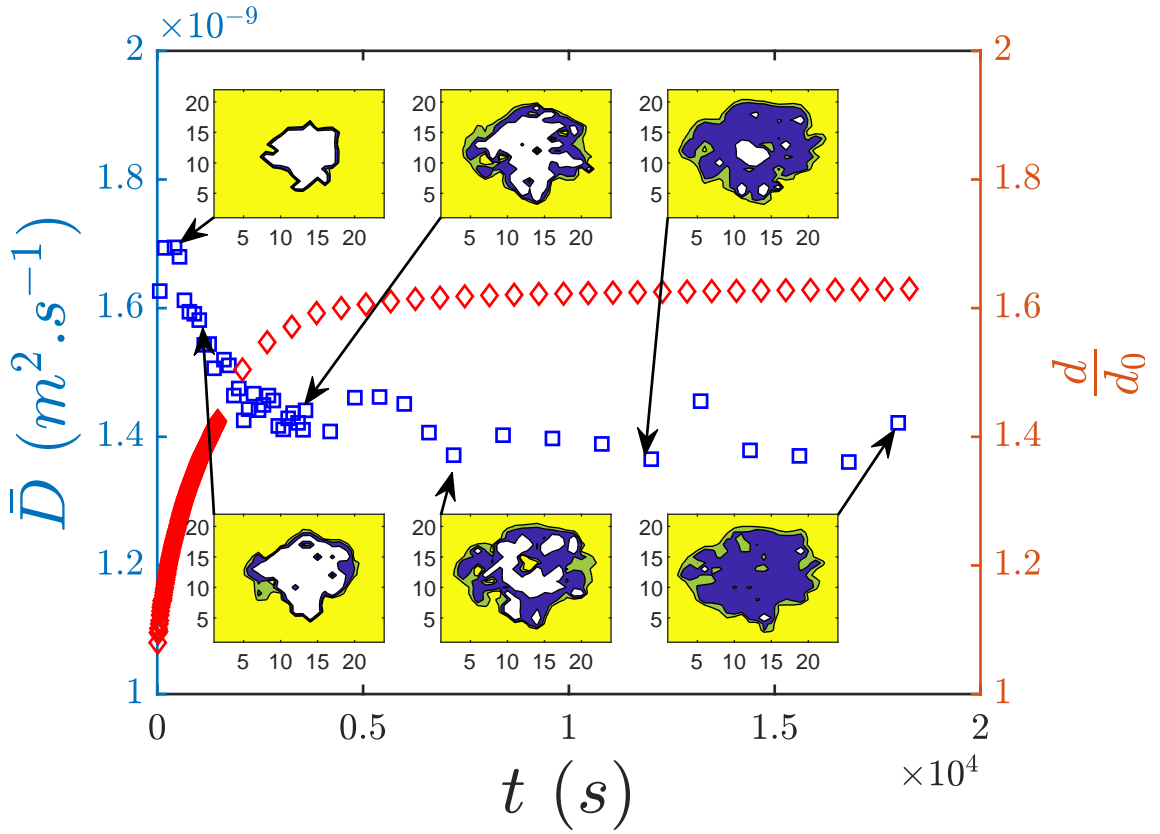


Figure 7: Time evolution of the mean diffusion coefficient \bar{D} and the normalized diameter d/d_0 during a swelling event. Images correspond to diffusion coefficient maps at different times. Each color is associated with a range of diffusion coefficients: $\bar{D} > 1.8 \times 10^{-9} \text{ m}^2 \cdot \text{s}^{-1}$ (yellow), $1.5 \times 10^{-9} < \bar{D} < 1.8 \times 10^{-9} \text{ m}^2 \cdot \text{s}^{-1}$ (green), $0.8 \times 10^{-9} < \bar{D} < 1.5 \times 10^{-9} \text{ m}^2 \cdot \text{s}^{-1}$ (blue), $\bar{D} < 0.8 \times 10^{-9} \text{ m}^2 \cdot \text{s}^{-1}$ (white).

168 d_0^2/\bar{D} is the characteristic timescale for diffusion of water through the particle and α^{-1} the ratio between particles and
 169 water densities ($\alpha = 0.7246 \pm 0.05$ in our experiments). The evolution of the re-scaled particle diameter is given by
 170 $d^* = (d(t) - d_0)/(d_{max} - d_0)$, where d_0 and d_{max} are the initial and the final diameters of the particle, respectively,
 171 and are extracted from experimental data. Comparisons between the experimental data and the usual models used in
 172 the literature (see Tab. 2) are presented in Fig. 8.

173 The models of Buchholz et al. (1998) and Sweijen et al. (2017a) are purely diffusive models, without any free
 174 parameters in our case. These two models predict a much faster swelling than that observed experimentally. In fact,
 175 the characteristic swelling time in these models is related to the diffusing time $d_0^2/4\bar{D} \approx 10^3$ s, which is an order of
 176 magnitude smaller than what is measured experimentally. This result suggests that swelling is influenced by water
 177 uptake at the surface of the grain and not only by diffusion, as evidenced by the best quality of fit for Sweijen et al.
 178 (2017b) and Omidian et al. (1998) models. The only free parameter of these models, k , corresponds to the inverse of
 179 a characteristic absorption time at the surface of the grains, whose values are $k = 3.29 \cdot 10^{-4} \text{ s}^{-1}$ and $k = 2.15 \cdot 10^{-4}$

Table 2

Swelling models from the literature used for comparison with experimental data. $\alpha = \rho_w/\rho_s$ is the ratio between the water and particle densities.

Models	Parameters	References
$\frac{d(t)}{d_0} = \frac{d_{max}}{d_0-1}(1 - e^{-kt})$	k free parameter	Omidian et al. (1998)[29]
$\frac{d(t)}{d_0} = [1 - \theta_{max}(e^{-kt} - 1)]^{-1/3}$	$\theta_{max} = 1 - \left(\frac{d_0}{d_{max}}\right)^3$, k free parameter	Sweijen et al. (2017b)[40]
$d'(t) = \frac{4\pi^2 d_0 \bar{D}}{3\alpha d^2(t)} \left[Q_{max} - \alpha \left(\frac{d(t)}{d_0} \right)^2 + \alpha - 1 \right]$	$\alpha = 0.7246$, $Q_{max} = 3.62$, $\bar{D} = 1.4 \cdot 10^{-9} \text{ m}^2 \cdot \text{s}^{-1}$	Buchholz et al. (1998)[5]
$d'(t) = \frac{4\bar{D}}{\alpha d(t)} \frac{Q_{max} - \alpha \left(\frac{d(t)}{d_0} \right)^3 + \alpha - 1}{\alpha(d(t)/d_0)^3 - \alpha + 1}$	$\alpha = 0.7246$, $Q_{max} = 3.62$, $D = 1.4 \cdot 10^{-9} \text{ m}^2 \cdot \text{s}^{-1}$	Sweijen et al.(2017a)[39]

180 s^{-1} for the Sweijen et al. (2017b) and Omidian et al.(1998) models, respectively.

181 In our case, $K = kd_0^2/4\bar{D} \ll 1$ is the only dimensionless group of the problem and is related to a water uptake-
 182 limiting swelling behavior. This can be explained by the existence of a layer near the surface of the particles where
 183 the diffusion properties are largely modified. This hypothesis is supported by the observation of an inhomogeneity of
 184 the diffusion properties in a crown of thickness $\approx 300 \mu\text{m}$ (see Fig. 7) and by recent works on the internal structure
 185 of couscous [16], where the authors show that the kinetics of the changes to the physicochemical characteristics of the
 186 grains during the cooking and the drying stages can contribute to generating heterogeneities in the couscous grains. In
 187 fact, the internal structure of agglomerates results from the spatial arrangement and the agglomeration of the primary
 188 particles induced by capillary forces and starch gelatinization at the surface, which in turn modify diffusion properties.
 189 The chemical composition of the powder, as well as the production process, need to be highlighted to understand the
 190 complexity of the swelling mechanisms occurring in this “real” food powder:

191 - According to Debet and Gidley (2006) [7], the presence of surface components (i.e. residual proteins, lipids) impacts
 192 the granular swelling of starch (rate and extent), particularly for two of the most commonly used starches (maize and
 193 wheat). The presence of these components is far from negligible in couscous powders (see table 1) and may enhance
 194 the intricacy of the powder swelling.

195 - During industrial production, a cooking stage inducing partial melting and merging of the particles is performed in
 196 order to transform wet agglomerates into more plastic and stable grains. During this step, a part of the starch (i.e.
 197 the main component of couscous) is gelatinized, amylose-lipid complexes are created and proteins (i.e. gluten) are
 198 insolubilized. These very complex phenomena are not identical throughout the particle, meaning that some parts of
 199 the grain may be more modified than others. This may be particularly true at the particle surface, explaining disparities
 200 observed between mathematical models and our observations. Also, the extent of starch gelatinization after the cooking
 201 stage was found to vary in the ratio from one (Debbouz and Donnelly (1996)[6]) to two (Bellocq et al. (2018)[3]) and
 202 may also impact particle swelling behavior.

203 It is important to note that the Omidian et al.(1998) model was initially interpreted in the literature as a purely

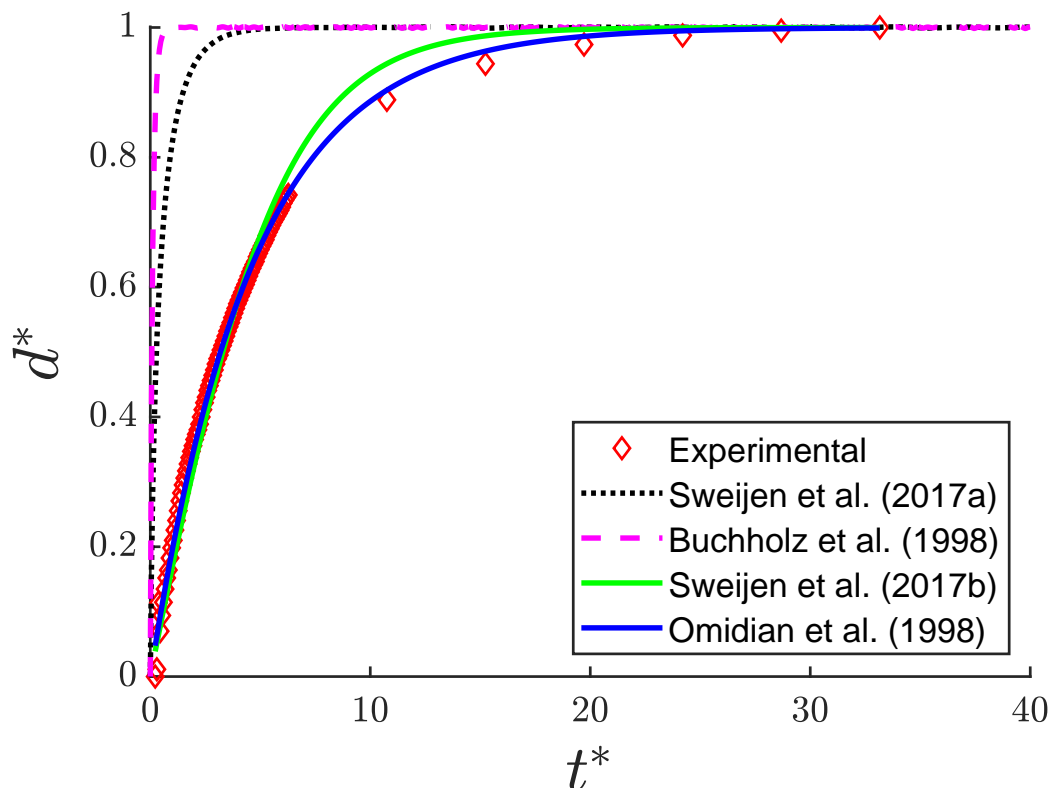


Figure 8: Evolution of the normalized diameter d^* as a function of the normalized time t^* . Experimental data are compared to different swelling models extracted from the literature. Experimental data are the mean out of 10 independent experiments. The Omidian et al. (1998) and Sweijen et al. (2017b) models are fitted to experimental data with only one free parameter ($R^2 = 0.9809$ and 0.9652 , respectively). There is no free parameter for the other models presented.

204 diffusing model. Authors have related it to a Voigt rheological model that accounts for the immediate elastic and
 205 delayed viscous strain responses due to gelatinization within the grain. Our result shows that this model also captures
 206 the swelling dynamics of couscous grains well in our experiments and can be employed as a law for water uptake at
 207 the particle's surface, as suggested in the recent works of Sweijen et al.[39, 40].

208 **4. Conclusions**

209 In this paper, the swelling properties of couscous grains under liquid saturation conditions at ambient temperature
 210 have been studied. It has been shown that a recent time-resolved MRI technique can be an efficient tool to investigate
 211 water penetration inside granular materials in food.

212 The majority of swelling models proposed in the literature are based either on the assumption of a diffusive dynam-
 213 ics with an assumed constant diffusion coefficient, or on water uptake-limiting dynamics via absorption at the particle
 214 surface.

215 By monitoring both the evolution of the particle diameter and the apparent diffusion coefficient of the liquid within
 216 the grain, [it has been shown](#) that a first-order kinetic model accounting for the dynamics of water capture at the surface
 217 of the particles allows to describe the growth of the particle size over time. The results suggest that the swelling
 218 dynamics is a water uptake-limiting mechanism because of the existence of a gelatinous layer at the grain surface
 219 formed during the manufacturing process, as previously reported in the literature.

220 MRI offers new perspectives for in situ monitoring of the water intake and water distribution of couscous grains.
 221 This technique may be generalized to others steps occurring during couscous formulation, for example to assess starch
 222 gelatinization or retrogradation phenomena.

223 5. Bibliography

224 CRediT authorship contribution statement

225 **Sébastien KIESGEN DE RICHTER:** Conceptualization, Methodology, Formal analysis, Investigation, Writing -
 226 Original draft, Supervision, Funding acquisition. **Naïma GAUDEL:** Methodology, Validation, Investigation, Writing
 227 - Original draft, Visualization. **Claire GAIANI:** Resources, Writing - Original draft, Supervision, Funding acquisition.
 228 **Arthur PASCOT:** Software, Writing - Original draft. **Maude FERRARI:** Methodology, Software, Validation,
 229 Investigation, Visualization. **Mathieu JENNY:** Software, Formal analysis, Investigation.

230 References

- 231 [1] Bell, C.L., Peppas, N.A., 1996. An apparatus to measure polymer swelling under load. *International journal of pharmaceutics* 134, 167–172.
- 232 [2] Bellocq, B., Cuq, B., Ruiz, T., Duri, A., Cronin, K., Ring, D., 2018a. Impact of fluidized bed granulation on structure and functional properties
 233 of the agglomerates based on the durum wheat semolina. *Innovative Food Science & Emerging Technologies* 45, 73–83.
- 234 [3] Bellocq, B., Ruiz, T., Cuq, B., 2018b. Contribution of cooking and drying to the structure of couscous grains made from durum wheat
 235 semolina. *Cereal chemistry* 95, 646–659.
- 236 [4] Bennethum, L.S., Cushman, J.H., 1996. Multiscale, hybrid mixture theory for swelling systems—i: balance laws. *International Journal of
 237 Engineering Science* 34, 125–145.
- 238 [5] Buchholz, F.L., Graham, A.T., 1998. Modern superabsorbent polymer technology. John! Wiley & Sons, Inc, 605 Third Ave, New York, NY
 239 10016, USA, 1998. 279 .
- 240 [6] Debbouz, A., Donnelly, B., 1996. Process effect on couscous quality. *Cereal chemistry (USA)* .
- 241 [7] Debet, M.R., Gidley, M.J., 2006. Three classes of starch granule swelling: Influence of surface proteins and lipids. *Carbohydrate Polymers*
 242 64, 452–465.
- 243 [8] Desai, P.M., Liew, C.V., Heng, P.W.S., 2016. Review of disintegrants and the disintegration phenomena. *Journal of pharmaceutical sciences*
 244 105, 2545–2555.
- 245 [9] Diersch, H.J.G., Clausnitzer, V., Myrnyy, V., Rosati, R., Schmidt, M., Beruda, H., Ehrnsperger, B.J., Virgilio, R., 2010. Modeling unsaturated
 246 flow in absorbent swelling porous media: Part 1. theory. *Transport in Porous Media* 83, 437–464.

- 247 [10] Espinoza, D.N., Vandamme, M., Pereira, J.M., Dangla, P., Vidal-Gilbert, S., 2014. Measurement and modeling of adsorptive–poromechanical
248 properties of bituminous coal cores exposed to co₂: Adsorption, swelling strains, swelling stresses and impact on fracture permeability.
249 International Journal of Coal Geology 134, 80–95.
- 250 [11] Esteves, L.P., 2011. Superabsorbent polymers: On their interaction with water and pore fluid. Cement and Concrete Composites 33, 717–724.
- 251 [12] Faroongsarng, D., Peck, G.E., 1994. The swelling & water uptake of tablets iii: moisture sorption behavior of tablet disintegrants. Drug
252 development and industrial pharmacy 20, 779–798.
- 253 [13] Forny, L., Marabi, A., Palzer, S., 2011. Wetting, disintegration and dissolution of agglomerated water soluble powders. Powder Technology
254 206, 72–78.
- 255 [14] Freudig, B., Hogekamp, S., Schubert, H., 1999. Dispersion of powders in liquids in a stirred vessel. Chemical Engineering and Processing:
256 Process Intensification 38, 525–532.
- 257 [15] Gaiani, C., Banon, S., Scher, J., Schuck, P., Hardy, J., 2005. Use of a turbidity sensor to characterize micellar casein powder rehydration:
258 Influence of some technological effects. Journal of dairy Science 88, 2700–2706.
- 259 [16] Hafsa, I., Cuq, B., Kim, S.J., Le Bail, A., Ruiz, T., Chevallier, S., 2014. Description of internal microstructure of agglomerated cereal powders
260 using x-ray microtomography to study of process–structure relationships. Powder technology 256, 512–521.
- 261 [17] Hammami, R., Sissons, M., 2020. Durum wheat products, couscous, in: Wheat Quality For Improving Processing And Human Health.
262 Springer, pp. 347–367.
- 263 [18] Hebrard, A., Oulahna, D., Galet, L., Cuq, B., Abecassis, J., Fages, J., 2003. Hydration properties of durum wheat semolina: influence of
264 particle size and temperature. Powder Technology 130, 211–218.
- 265 [19] Hogekamp, S., Schubert, H., 2003. Rehydration of food powders. Food Science and Technology International 9, 223–235.
- 266 [20] Huang, C., Becker, M.F., Keto, J.W., Kovar, D., 2007. Annealing of nanostructured silver films produced by supersonic deposition of nanopar-
267 ticles. Journal of Applied Physics 102, 054308.
- 268 [21] Huyghe, J.M., Janssen, J.D., 1997. Quadriphasic mechanics of swelling incompressible porous media. International Journal of Engineering
269 Science 35, 793–802.
- 270 [22] Ji, J., Cronin, K., Fitzpatrick, J., Fenelon, M., Miao, S., 2015. Effects of fluid bed agglomeration on the structure modification and reconstitution
271 behaviour of milk protein isolate powders. Journal of Food Engineering 167, 175–182.
- 272 [23] Kovrlija, R., Rondeau-Mouro, C., 2017. Multi-scale nmr and mri approaches to characterize starchy products. Food chemistry 236, 2–14.
- 273 [24] Kyaw Hla, P., Hogekamp, S., 1999. Wetting behaviour of instantized cocoa beverage powders. International journal of food science &
274 technology 34, 335–342.
- 275 [25] Markl, D., Wang, P., Ridgway, C., Karttunen, A.P., Chakraborty, M., Bawuah, P., Pääkkönen, P., Gane, P., Ketolainen, J., Peiponen, K.E.,
276 et al., 2017. Characterization of the pore structure of functionalized calcium carbonate tablets by terahertz time-domain spectroscopy and
277 x-ray computed microtomography. Journal of Pharmaceutical Sciences 106, 1586–1595.
- 278 [26] Mitchell, W.R., Forny, L., Althaus, T.O., Niederreiter, G., Palzer, S., Hounslow, M.J., Salman, A.D., 2015. Mapping the rate-limiting regimes
279 of food powder reconstitution in a standard mixing vessel. Powder Technology 270, 520–527.
- 280 [27] Murad, M.A., Cushman, J.H., 1996. Multiscale flow and deformation in hydrophilic swelling porous media. International Journal of Engi-
281 neering Science 34, 313–338.
- 282 [28] O'Mahony, J.A., McSweeney, P.L., 2016. Advanced dairy chemistry. volume 1B: Proteins: Applied Aspects. Springer.
- 283 [29] Omidian, H., Hashemi, S., Sammes, P., Meldrum, I., 1998. A model for the swelling of superabsorbent polymers. Polymer 39, 6697–6704.
- 284 [30] Pan, Z., Connell, L.D., 2012. Modelling permeability for coal reservoirs: a review of analytical models and testing data. International Journal

- 285 of Coal Geology 92, 1–44.
- 286 [31] Parker, A., Vigouroux, F., Reed, W.F., 2000. Dissolution kinetics of polymer powders. *AIChE journal* 46, 1290–1299.
- 287 [32] Romero, E., DELLA VECCHIA, G., Jommi, C., 2011. An insight into the water retention properties of compacted clayey soils. *Géotechnique*
288 61, 313–328.
- 289 [33] Rudnic, E., Rhodes, C., Welch, S., Bernardo, P., 1982. Evaluations of the mechanism of disintegrant action. *Drug Development and Industrial*
290 *Pharmacy* 8, 87–109.
- 291 [34] Schubert, H., 1993. Instantization of powdered food products. *International Chemical Engineering* 33, 28–45.
- 292 [35] Schuck, P., Jeantet, R., Dolivet, A., 2012. Analytical methods for food and dairy powders. John Wiley & Sons.
- 293 [36] Siepmann, J., Siepmann, F., 2008. Mathematical modeling of drug delivery. *International journal of pharmaceutics* 364, 328–343.
- 294 [37] Soundaranathan, M., Vivattanaseth, P., Walsh, E., Pitt, K., Johnston, B., Markl, D., 2020. Quantification of swelling characteristics of
295 pharmaceutical particles. *International Journal of Pharmaceutics* 590, 119903.
- 296 [38] Stejskal, E.O., Tanner, J.E., 1965. Spin diffusion measurements: spin echoes in the presence of a time-dependent field gradient. *The journal*
297 *of chemical physics* 42, 288–292.
- 298 [39] Sweijen, T., Chareyre, B., Hassanzadeh, S., Karadimitriou, N., 2017a. Grain-scale modelling of swelling granular materials; application to
299 super absorbent polymers. *Powder Technology* 318, 411–422.
- 300 [40] Sweijen, T., van Duijn, C., Hassanzadeh, S., 2017b. A model for diffusion of water into a swelling particle with a free boundary: Application
301 to a super absorbent polymer particle. *Chemical Engineering Science* 172, 407–413.
- 302 [41] Takhar, P.S., 2014. Unsaturated fluid transport in swelling poroviscoelastic biopolymers. *Chemical Engineering Science* 109, 98–110.
- 303 [42] Tanner, J.E., 1970. Use of the stimulated echo in nmr diffusion studies. *The Journal of Chemical Physics* 52, 2523–2526.
- 304 [43] Tester, R.F., Morrison, W.R., 1990. Swelling and gelatinization of cereal starches. ii. waxy rice starches. *Cereal Chem* 67, 558–563.
- 305 [44] Yeh, A.I., Li, J.Y., 1996. A continuous measurement of swelling of rice starch during heating. *Journal of Cereal Science* 23, 277–283.
- 306 [45] Zhao, N., Augsburger, L.L., 2005. The influence of swelling capacity of superdisintegrants in different ph media on the dissolution of
307 hydrochlorothiazide from directly compressed tablets. *AAPS pharmscitech* 6, E120–E126.

Swelling of couscous grains under saturated conditions

Sébastien KIESGEN DE RICHTER,Naïma GAUDEL,Claire GAIANI,Arthur PASCOT,Maude FERRARI,Mathieu JENNY

- MRI is an effective tool to investigate water distribution in granular food materials
- Water diffusion coefficient in grains is heterogeneously distributed in space
- Classical diffusive models from the literature cannot predict swelling dynamics
- Results suggest that the swelling dynamics is a water uptake-limiting mechanism

Dear Editor,

This manuscript has not yet been published elsewhere and it is not under consideration by another journal. All authors have approved the manuscript and have agreed to submit it to Journal of Food Engineering. All authors have also read and adhered to the Statement of Ethical Standards for manuscript submitted to Journal of Food Engineering.

Finally, the authors have no known conflicts of interest.

Graphical Abstract

Swelling of couscous grains under saturated conditions

Sébastien KIESGEN DE RICHTER, Naïma GAUDEL, Claire GAIANI, Arthur PASCOT, Maude FERRARI, Mathieu JENNY

